2M14

NASA TECHNICAL NOTE

NASA TN D-7414

NASA TN D-7414

OPTICAL ANALYSIS OF A COMPOUND QUASI-MICROSCOPE FOR PLANETARY LANDERS

by Stephen D. Wall, Ernest E. Burcher, and Friedrich O. Huck

Langley Research Center
Hampton, Va. 23665

NATIONAL AERONAUTICS AND SPACE ADMINISTRATION • WASHINGTON, D. C. • APRIL 1974

1. Report No.	2. Government Accession No.	3. Recipient's Catalog No.
NASA TN D-7414		

4. Title and Subtitle	5. Report Date
OPTICAL ANALYSIS OF A COMPOUND QUASI-MICROSCOPE FOR PLANETARY LANDERS	April 1974
	6. Performing Organization Code
7. Author(s)	8. Performing Organization Report No.
Stephen D. Wall, Ernest E. Burcher, and Friedrich O. Huck	L-9001
	10. Work Unit No.
9. Performing Organization Name and Address	502-03-52-00
NASA Langley Research Center	11. Contract or Grant No.
Hampton, Va. 23665	
	13. Type of Report and Period Covered
12. Sponsoring Agency Name and Address	Technical Note
National Aeronautics and Space Administration	14. Sponsoring Agency Code
Washington, D.C. 20546	

15. Supplementary Notes

16. Abstract

Current state-of-the-art planetary lander cameras can resolve surface detail on the order of 1 mm at best. Microscopes which have been investigated and proposed for planetary-lander missions could resolve details of about 0.2 μm, but only with very complex instrumentation. In order to bridge this gap, a quasi-microscope concept, consisting of a facsimile camera augmented with an auxiliary lens as a magnifier, was introduced and analyzed in NASA TN D-7129. The performance achievable with this concept was primarily limited by a trade-off between resolution and object field; this approach leads to a limiting resolution of 20 μm when used with the Viking lander camera (which has an angular resolution of 0.04^{o}).

An optical system is analyzed here which includes a field lens between camera and auxiliary lens to overcome this limitation. It is found that this system, referred to as a compound quasi-microscope, can provide improved resolution (to about 2 μm) and a larger object field. However, this improvement is made at the expense of increased complexity, special camera design requirements, and tighter tolerances on the distances between optical components.

17. Key Words (Suggested by Author(s))	18. Distribution Statement
Planetary lander cameras Remote microscope Facsimile camera Optical analysis	Unclassified – Unlimited STAR Category 23

19. Security Classif. (of this report)	20. Security Classif. (of this page)	21. No. of Pages	22. Price*
Unclassified	Unclassified	35	$3.25

*For sale by the National Technical Information Service, Springfield, Virginia 22151

OPTICAL ANALYSIS OF A COMPOUND QUASI-MICROSCOPE FOR PLANETARY LANDERS

By Stephen D. Wall, Ernest E. Burcher, and Friedrich O. Huck
Langley Research Center

SUMMARY

Current state-of-the-art planetary lander cameras can resolve surface detail on the order of 1 mm at best. Microscopes which have been investigated and proposed for planetary-lander missions could resolve details of about 0.2 μm, but only with very complex instrumentation. In order to bridge this gap, a quasi-microscope concept, consisting of a facsimile camera augmented with an auxiliary lens as a magnifier, was introduced and analyzed in NASA TN D-7129. The performance achievable with this concept was primarily limited by a trade-off between resolution and object field; this approach leads to a limiting resolution of 20 μm when used with the Viking lander camera (which has an angular resolution of 0.04^{o}).

An optical system is analyzed here which includes a field lens between camera and auxiliary lens to overcome this limitation. It is found that this system, referred to as a compound quasi-microscope, can provide improved resolution (to about 2 μm) and a larger object field. However, this improvement is made at the expense of increased complexity, special camera design requirements, and tighter tolerances on the distances between optical components.

INTRODUCTION

Visual imaging of the terrain surrounding a lunar or planetary lander is generally accepted to be of primary importance, as demonstrated by the U.S.S.R. in the Luna (refs. 1 and 2) and Lunakhod (ref. 3) missions, and by the U.S.A. in the Surveyor (ref. 4) and Viking (ref. 5) missions. Capabilities of the imaging systems on these spacecraft have been limited to resolvable details of about 1 to 10 mm, although better resolution would have been highly desirable. To obtain better resolution of selected surface samples, microscopes have been proposed which are capable of resolving details down to 0.4 μm. (See refs. 6, 7, and 8.) However, these microscopes require complex instrumentation and have never been accepted for a space mission.

In order to bridge the gap between the resolution obtainable directly with current state-of-the-art lander cameras and the higher resolution obtainable only with complex microscopes, a concept consisting of a lander camera augmented with an auxiliary lens as a magnifier, referred to as a quasi-microscope, was introduced and analyzed in reference 9. A major advantage of this concept is the simplicity with which it can be implemented. Although it is generally desirable to place this auxiliary lens close to the camera in order to obtain a wide object field, the distance between camera and auxiliary lens is not critical and is independent of the auxiliary- and camera-lens focal lengths. The major disadvantage of this concept is the trade-off necessary between resolution and object field. Resolutions approaching 20 μm can be obtained only for very small usable object fields and even then only with very low f-number auxiliary lenses, which, in turn, lead to difficult lens design requirements.

This paper investigates a compound quasi-microscope which reduces the performance constraint of the simple quasi-microscope by including a field lens between the auxiliary lens and the camera.

SYMBOLS

c	distance from auxiliary lens to camera lens, m
D	lens clear-aperture diameter, m
D_i	diameter of auxiliary-lens image, m
d	diameter of picture element (pixel), or resolution diameter, m
f	lens focal length, m
h	off-axis height, m
K	distance from field lens to scanning mirror, m
l	object or image distance from lens, m
Δl	depth of field or focus, m
m_t	transverse magnification

β camera instantaneous field of view (angular resolution), rad

Δ image misplacement, m (see fig. 9(a))

δ image-plane error, m (see fig. 6(a))

ϵ lens-misplacement error, m

θ off-axis angle, rad

ξ distance, m (see fig. 7(a))

Ω number of unvignetted picture elements (pixels) in central line scan

Subscripts:

a auxiliary lens

c camera lens

f field lens

A horizontal bar over a symbol represents the simple rather than the compound quasi-microscope design.

A prime represents the image rather than the object side of a lens.

A tilde over a variable indicates a conjugate due to some misplaced element.

ANALYSIS OF PERFORMANCE CHARACTERISTICS

This section reviews pertinent optical characteristics of the simple quasi-microscope cited in reference 9, reformulates optical performance characteristics when a field lens is added to make a compound quasi-microscope, and compares the performance of these two optical systems. Only thin lenses and first-order geometrical optics are considered. Requirements and constraints of the compound quasi-microscope are formulated in the next section.

Review of Quasi-Microscope Characteristics

A basic optical configuration of the quasi-microscope is illustrated in figure 1(a). The facsimile camera consists essentially of a radiometer and a scanning mechanism. The objective lens of the radiometer captures light and transmits it through a pinhole to a photosensor which transduces it into an electrical signal. The scanning mechanism generates vertical line scans by a nodding or rotating mirror and provides proper spacing between successive line scans by rotating the line-scan and radiometer assembly in azimuth. The performance parameters of the facsimile camera important to this analysis (presented in ref. 10) are instantaneous field of view, or angular resolution, given by

$$\beta = 2 \tan^{-1} \frac{d_c}{2l_c'} \approx \frac{d_c}{l_c'} \tag{1}$$

depth of focus, given by

$$\Delta l_c' = \frac{2l_c' d_c}{D_c\left[1 - \left(\frac{d_c}{D_c}\right)^2\right]} \approx \frac{2l_c' d_c}{D_c} = \frac{2\beta l_c'^2}{D_c} \tag{2}$$

and, similarly, depth of field, given by

$$\Delta l_c \approx \frac{2\beta l_c^2}{D_c} \tag{3}$$

The approximation assumes that $d_c \ll D_c$, which is generally the case.

In the simple quasi-microscope, the auxiliary lens is located remotely from the facsimile camera and forms a magnified image of the sample at infinity, which, in turn, is imaged by the facsimile camera.

The configuration of particular importance, and the only one considered in this section, is the one which achieves best resolution without imposing any special design requirements on the facsimile camera. In this configuration the object is placed at the focal point of the auxiliary lens (i.e., with $l_a = \bar{f}_a$) and the camera photosensor aperture is located at or near the focal point of the objective lens (i.e., $l_c' \cong \bar{f}_c'$).

The basic configuration is shown with the optical path unfolded in figure 1(b). (Thin lenses are shown as double-ended arrows throughout the paper.) For each lens, l is the object distance and l' is the image distance; f represents the focal length, and D is the clear-aperture diameter. Subscripts indicate the lens involved. The mirror-scanning

motion will be modeled by moving the photosensor pinhole and neglecting the angle scanned by the camera mirror.

The performance parameters of interest (from ref. 9) are transverse magnification given by

$$\bar{m}_t = \frac{\bar{f}_c}{\bar{f}_a} \tag{4}$$

picture-element (pixel) diameter, taken as a measure of the system's linear resolution, given by

$$\bar{d}_a = \frac{d_c}{\bar{m}_t} = \beta \bar{f}_a \tag{5}$$

depth of field, given by

$$\overline{\Delta l}_a = \frac{\Delta l'_c}{m_t^2} = \frac{2\beta}{D_c} \bar{f}_a^{\,2} \tag{6}$$

and the number of unvignetted picture elements (pixels) in the line scan which passes through the center of the field of view, given by

$$\bar{\Omega} = \frac{D_a - D_c}{c\beta} \tag{7}$$

The total number of unvignetted pixels per image is given by $\frac{\pi}{4} \bar{\Omega}^2$.

The analytical results for equations (5) to (7) are plotted in figure 2. It is assumed that the Viking lander camera (see table I) is used and that the auxiliary-lens f-number is unity $(\text{i.e.,}\ f_a = D_a)$.

TABLE I.- ASSUMED DESIGN PARAMETERS

Viking lander camera (ref. 5):	
Instantaneous field of view, β, deg	0.04
Objective lens clear-aperture diameter, D_c, cm	0.95
Objective lens focal length, f_c, cm	5.3
Distance from lens to scanning mirror, K', cm	3.5
Auxiliary lens:	
Focal length, f_a, cm	3.0
Distance to camera lens, c, cm	100

Formulation of Compound Quasi-Microscope Characteristics

A major disadvantage of the simple quasi-microscope design is its small number of unvignetted pixels. This disadvantage may be overcome to a significant extent by adding a field lens between auxiliary and camera lens, as shown in figure 3(a). The purpose of the field lens is to direct light from the auxiliary lens into the camera lens and thereby increase the unvignetted field. To accomplish this, the auxiliary lens must form a real image. The field lens should be placed in this image plane, and the camera lens must be properly focused on this image.

The compound quasi-microscope configuration is shown with the optical path unfolded in figure 3(b). For the present, the mirror-scanning motion will be modeled by moving the photosensor pinhole as before. This approximation will be removed later.

If the field lens is to relay the magnified image formed by the auxiliary lens to the camera, then the field lens must be located where the image is formed (and where, incidentally, it adds no magnification to the system). Then, $l'_a = l_f$ and $l'_f = l_c$, as shown in figure 3(b). As for the simple quasi-microscope, the performance parameters of interest are transverse magnification, pixel (or resolution) diameter, depth of field, and number of unvignetted pixels.

Transverse magnification. - Since the field lens adds no magnification, the optical-system magnification is simply the product of the auxiliary-lens and camera-lens magnifications given by

$$m_t = (m_{ta})(m_{tc}) = \frac{l'_a l'_c}{l_a l_c} = \frac{l_f l'_c}{l_a l'_f} \tag{8a}$$

In order to change the magnification m_t and at the same time keep the object distance and final image distance constant, the powers of both camera and auxiliary lenses have to be changed. This effect appears in equation (8a) through a change in l_f and l'_f. In order to alter l_f and l'_f simultaneously though, either the distance c must change or the field-lens power must be adjusted so that c can be held constant. In order to compare the quasi-microscope effectively with the compound quasi-microscope, it is more convenient to keep the distance c constant and write m_t as a function of l'_f. Thus,

$$m_t = \left(\frac{c - l'_f}{l_a}\right)\frac{l'_c}{l'_f} = \frac{l'_c}{l_a}\left(\frac{1 - \frac{l'_f}{c}}{\frac{l'_f}{c}}\right) \tag{8b}$$

Resolution.- The pixel diameter, or resolution diameter, is given by

$$d_a = \frac{d_c}{m_t} = \frac{d_c}{l'_c} l_a \left(\frac{\frac{l'_f}{c}}{1 - \frac{l'_f}{c}} \right) \tag{9a}$$

This equation may be rewritten in terms of the facsimile-camera angular resolution (see eq. (1)) as

$$d_a = \beta l_a \left(\frac{\frac{l'_f}{c}}{1 - \frac{l'_f}{c}} \right) \tag{9b}$$

Depth of field.- The depth of field is given by

$$\Delta l_a = \frac{\Delta l_c}{m_t^2} = \Delta l'_c \left(\frac{l_a}{l'_c} \right)^2 \left(\frac{\frac{l'_f}{c}}{1 - \frac{l'_f}{c}} \right)^2 \tag{10a}$$

Substitution from equations (1) and (2) yields

$$\Delta l_a = \frac{2\beta}{D_c} l_a^2 \left(\frac{\frac{l'_f}{c}}{1 - \frac{l'_f}{c}} \right)^2 \tag{10b}$$

Number of unvignetted pixels.- Figure 3(b) shows the imaging situation for an off-axis pixel. For any field lens of finite size, light coming from pixels beyond some off-axis angle will miss the field lens and therefore will not be relayed to the camera; these pixels are called vignetted pixels. Vignetting begins when the off-axis distance in the camera h' is such that

$$\frac{h' l'_f}{l'_c} = \frac{D_f}{2}$$

that is, when the intermediate image point falls off the edge of the field lens. (See fig. 3(b).) Consequently, the total number of unvignetted pixels per line scan through the center of the auxiliary lens is given by

$$\Omega = \frac{2h'}{\beta l'_c} = \frac{D_f}{\beta l'_f} \tag{11}$$

Comparison of Simple and Compound Quasi-Microscope

Performance Characteristics

Comparing equations (4), (5), and (6) with equations (8b), (9b), and (10b) allows the performance of the compound design to be expressed as a function of the simple design:

$$m_t = \bar{m}_t \left(\frac{l'_c}{\bar{f}_c} \frac{f_a}{l_a} \right) \left(\frac{1 - \frac{l'_f}{c}}{\frac{l'_f}{c}} \right) \tag{12}$$

$$d_a = \bar{d}_a \left(\frac{l_a}{\bar{f}_a} \right) \left(\frac{\frac{l'_f}{c}}{1 - \frac{l'_f}{c}} \right) \tag{13}$$

$$\Delta l_a = \overline{\Delta l}_a \left(\frac{l_a}{\bar{f}_a} \right)^2 \left(\frac{\frac{l'_f}{c}}{1 - \frac{l'_f}{c}} \right)^2 \tag{14}$$

As the field-lens position l'_f/c changes, the image and object distances l'_c and l_a also change.

If one imagines a simple quasi-microscope which has object and image distances (given by f_a and f_c) equal to those of a compound design (l_a and l'_c) with some fixed value of l'_f/c, then the parenthetical expressions in equations (12), (13), and (14) are all unity, and direct comparisons can be made between the two systems by use of the equations

$$m_t = \bar{m}_t \left(\frac{1 - \frac{l'_f}{c}}{\frac{l'_f}{c}} \right) \tag{15}$$

$$d_a = \bar{d}_a \left(\frac{\frac{l'_f}{c}}{1 - \frac{l'_f}{c}} \right) \tag{16}$$

$$\Delta l_a = \overline{\Delta l}_a \left(\frac{\frac{l'_f}{c}}{1 - \frac{l'_f}{c}} \right)^2 \tag{17}$$

The numbers of unvignetted pixels for the two systems are not directly comparable, since the addition of a field lens completely changes the dependence of vignetting. In fact, the principal advantage of using a field lens in this (as in any) optical system is that the field covered is no longer a function of the diameters of either of the imaging lenses. This is extremely important, since the size of the aperture stop is determined by these lenses, and the aperture stop limits the amount of light that can be gathered by the system. With the addition of the field lens, it is possible to control the field coverage and the light-gathering ability of the quasi-microscope separately. This general conclusion is somewhat constrained by the camera mirror-scanning motion as formulated in the following section. Disregarding this constraint here, it is convenient to rewrite equation (11) as a function of l'_f/c in the form

$$\Omega = \frac{D_f}{c\beta} \left(\frac{1}{\frac{l'_f}{c}} \right) \tag{18}$$

following a procedure similar to that used in equations (12) to (17).

The variation of these quantities with relative field-lens position, given by the ratio l'_f/c, is shown in figure 4. Notice that the quasi-microscope illustrated at the top of figure 4 is reversed from the previous illustrations to correspond with the graphs below it. In figure 4(a), vertical axes represent the relative gain over the equivalent simple quasi-microscope, where "equivalent" is taken to mean equal object and image conjugates in the sense of the previous discussion. Notice, for example, that when the field lens is placed half-way between the camera and auxiliary lens, the gain is unity in each case, and there is no advantage in using the compound design with respect to resolution, magnification, or depth of field. The number of unvignetted pixels per line scan (Ω) is given in figure 4(b) in terms of $D_f/c\beta$.

In summary, these graphs lead to three important conclusions about the use of a field lens:

(1) The major constraint imposed on the simple quasi-microscope performance by the trade-off necessary between the best resolution (requiring a small auxiliary-lens focal length) and the largest unvignetted field (requiring a large auxiliary-lens diameter) is apparently lifted, thus allowing both improved resolutions and larger numbers of unvignetted pixels.

(2) Both magnification and number of unvignetted pixels increase – but depth of field decreases – as the field lens is moved toward the camera.

(3) Increase in magnification over the simple quasi-microscope can be obtained only if the field lens is placed closer than half-way to the camera, that is, if $l_f' \leq \frac{c}{2}$.

ANALYSIS OF CONSTRAINTS AND REQUIREMENTS

In the simple quasi-microscope design, no special focus requirements are imposed on the facsimile camera, and the distance between the auxiliary lens and the camera is not critical. In the compound design the facsimile camera sees a real image formed by the auxiliary lens at the field-lens location, thus imposing several requirements and constraints on the arrangement of the optical components and the camera design. As will be shown in this section, effects due to the rotating camera mirror can no longer be ignored, and the relative positioning of the various lenses becomes critical. The principal effect of these constraints is to place limits on the possible placements of the field lens, which, in turn, serves to limit the magnification, resolution, and field of view predicted in figure 4.

Scanning-Mirror Effects

The foregoing performance analysis has been based on an optical system which was unfolded about a scanning mirror positioned at a 45° angle, as illustrated in figure 5(a). An object point not located on the auxiliary-lens axis was, therefore, assumed to be imaged off-axis by the camera lens, and the photodetector was assumed to have moved mysteriously off-axis to record such a point.

In reality, however, as shown in figure 5(b), the quasi-microscope images an object point quite differently. The image point located at an angle θ to the auxiliary-lens axis is made to fall on a photodetector, which is located on the camera-lens axis by rotating the scanning mirror (through an angle $\theta/2$). Consequently, in order to unfold the system correctly about the scanning-mirror axis, such unfolding must be done differently for each field angle, as is shown in figure 5(b).

The performance of the compound quasi-microscope predicted in figure 4 is still valid, but it is now constrained in two ways. First, the camera will not be in geometric focus at all field angles. In particular, at the field angle θ of figure 5(b) the final image is located at point B, whereas an on-axis point would be imaged at point A. Second, for any field angle except zero, the field lens will not be coaxial with the camera lens and, therefore, cannot place the auxiliary-lens image in the center of the camera lens. As a result, vignetting can occur if the camera-lens aperture and auxiliary-lens aperture are not chosen carefully. These two constraints will now be considered in detail.

Camera depth of field.- As is illustrated in figure 6(a), the surface generated by the geometric focus of the facsimile camera is a section of a sphere. At typical object distances beyond 1 or 2 meters, the curvature of this spherical section is contained within the camera depth of field and is unimportant. However, for the short camera-to-object distances in the compound quasi-microscope, this may not always be true.

The distance between the curved-object field and a planar image which is in focus at the optical axis is labeled δ in figure 6(a). At the edge of the field lens δ is given by

$$\delta^2 + 2K\delta = \left(\frac{D_f}{2}\right)^2$$

where K is the distance between field lens and mirror axis of rotation. Generally, $\delta \ll 2K$ which leads to

$$\delta = \frac{D_f^2}{8K} \tag{19}$$

The constraint now becomes that δ be within the depth of field Δl_c of the camera; that is,

$$\Delta l_c \geqq \delta \tag{20a}$$

Substituting equations (3) and (19) for Δl_c and δ, respectively, and letting $l_c = l_f'$ and $K' = l_f' - K$ yields

$$\left(\frac{l_f'}{c}\right)^3 - \frac{K'}{c}\left(\frac{l_f'}{c}\right)^2 - \left(\frac{D_f}{c}\right)^2\left(\frac{D_c}{c}\right)\left(\frac{1}{16\beta}\right) \geqq 0 \tag{20b}$$

The values of l_f'/c for which the left side of equation (20b) becomes zero serve as a limit for possible field-lens locations. These are plotted in figure 6(b) as a function of K'/c for typical values of D_f, D_c, and β.

Vignetting.- The aperture stop of an optical system is defined to be that aperture which ultimately limits the cone of light coming from an object point. The aperture stop of the compound quasi-microscope could conceivably be determined by either the auxiliary or camera lens (but not by the field lens since it lies at the vertex of the cone). In order to see which one of the two lenses determines the system aperture stop, let D_i be the image diameter of the auxiliary lens (with diameter D_a) as projected by the field lens onto the camera lens (with its diameter D_c); that is,

$$D_i = D_a \frac{l_f'}{l_f} = D_a \frac{l_f'}{c - l_f'} \tag{21}$$

Thus, for an on-axis object point, when $D_i < D_c$ the auxiliary lens determines the system aperture stop, and when $D_i > D_c$ the camera lens determines it.

For an off-axis object point, these two lens apertures will not have a common center, and some combination of D_i and D_c may often determine the aperture stop. Since the area of this stop will then depend on the off-axis angle, the light gathered by the system would be different at different field points. This situation, known as field vignetting, is undesirable since the light reaching the photosensor from the object then varies with the camera mirror-scanning angle.

In order to prevent field vignetting, the parameters D_a, l_f, and D_c must be chosen in one of two ways. These are illustrated in figure 7(a) as designs 1 and 2. In design 1, D_i is made small enough to lie always within D_c, even at the most off-axis field point allowed by the field lens. In design 2, D_i is made large enough for the camera-lens diameter D_c to lie always within it.

In particular, design 1 forces the auxiliary lens to act as the aperture stop for all field points. The constraint imposed on this design in order to avoid field vignetting may be formulated by projecting the auxiliary-lens image onto the camera lens, as shown in the enlarged view in figure 7(b). To avoid vignetting, this projection must not extend beyond the edge of the camera lens; that is,

$$\xi + K' \tan \theta + \frac{D_i}{2 \cos \theta} \leq \frac{D_c}{2} \tag{22}$$

where the distance ξ is illustrated in figure 7(a). It is shown in the appendix that if ϕ represents the angle shown in figure 7(a), then

$$\xi = \frac{D_i}{2} \frac{\tan\theta \sin\phi}{\cos(\theta + \phi)} \approx \frac{D_i}{2} \phi \tan\theta << K' \tan\theta$$

and ξ can be disregarded in equation (22).

Design 2 uses the camera lens as the aperture stop; hence, an advantage of design 2 is that the same noise-equivalent radiance is achieved for the quasi-microscope as for the unaided camera. The constraint for no field vignetting may be expressed as

$$\xi \tan\theta - K' \tan\theta + \frac{D_i}{2\cos\theta} \gtrless \frac{D_c}{2} \tag{23}$$

where the term $\xi \tan\theta$ can again be disregarded.

Considering design 1 further for small θ, equation (22) becomes

$$\frac{D_i}{2} + K' \tan\theta \leqq \frac{D_c}{2}$$

Substituting equation (21) for D_i and $D_f/2K$ for $\tan\theta$ results in

$$\frac{D_f}{c} \leqq \left[\frac{D_c}{c} - \left(\frac{\frac{l_f'}{c}}{1 - \frac{l_f'}{c}}\right)\frac{D_a}{c}\right]\left(\frac{\frac{l_f'}{c} - \frac{K'}{c}}{\frac{K'}{c}}\right) \tag{24a}$$

Likewise, the design 2 requirement formulated by equation (23) becomes

$$K' \tan\theta + \frac{D_c}{2} \leqq \frac{D_i}{2}$$

which leads to

$$\frac{D_f}{c} \leqq -\left[\frac{D_c}{c} - \left(\frac{\frac{l_f'}{c}}{1 - \frac{l_f'}{c}}\right)\frac{D_a}{c}\right]\left(\frac{\frac{l_f'}{c} - \frac{K'}{c}}{\frac{K'}{c}}\right) \tag{24b}$$

Figure 7(c) shows field-lens diameters and positions which satisfy equations (24) with assumed values of $D_c/c = 0.01$, $K'/c = 0.035$, and those values of D_a/c shown. The shaded areas indicate forbidden combinations of field-lens diameter and position.

From these graphs it can be seen that design 1 allows the field lens to be placed closer to the camera than does design 2, which can result in better resolution. (See fig. 4.) However, since the auxiliary lens is now the aperture stop of the quasi-microscope-camera system, the radiant power reaching the detector is reduced by the factor $\left(D_i/D_c\right)^2$.

It is important to note that the vignetting constraints shown in figure 7(c) are perhaps too severe. They indicate where vignetting starts at the edge of the field; but the vignetting will not be complete for some distance beyond these limits. The gradual darkening is predictable and could be compensated until some minimum signal-to-noise ratio is reached.

Camera Focus Requirements

It was shown previously that the in-focus facsimile-camera object plane is a spherical section (fig. 6(a)) which, because of its nearness to the camera, imposes a strict constraint on the field-lens placement. In addition, the nearness of the field lens also imposes a special focus requirement on the facsimile-camera design. To locate the required detector position l'_c, the thin-lens imaging equation may be written in the form

$$\frac{l'_c}{c} = \frac{f_c}{c}\left(\frac{\frac{l'_f}{c}}{\frac{l'_f}{c} - \frac{f_c}{c}}\right) \tag{25}$$

The variation of l'_c with the normalized field-lens position l'_f/c is shown in figure 8. The range of l'_c is somewhat arbitrarily limited to $2f_c$. Since the usual imaging detector is located close to the camera-lens focal plane (i.e., $l'_c \approx f_c$), a special requirement for $l'_c > 2f_c$ would have a very significant and undesirable impact on camera size.

Axial-Lens Misplacement

As has been pointed out, an important concern in the compound quasi-microscope, in contrast to the simple design, is that distances between lenses are critical. Since precise distances may be difficult to maintain on planetary-lander spacecraft, it is important to evaluate the effect of possible misplacements on overall system performance and to establish misplacement tolerances. The effects of misplacement of the auxiliary and field lens from the camera lens are considered separately.

Field lens.- Consider a small field-lens displacement ϵ_f from its proper location, as illustrated in figure 9(a). The image formed by the auxiliary lens will no longer be in the field lens but will be reimaged by the field lens. The resultant image will be located at a distance ϵ'_f from the field lens as given by

$$\epsilon_f' = \frac{1}{\frac{1}{f_f} - \frac{1}{\epsilon_f}} = \frac{\epsilon_f f_f}{\epsilon_f - f_f}$$

The total distance between the image seen by the camera (the second intermediate image) and the image expected by the camera (the image formed by the auxiliary lens alone) is given as

$$\Delta = \epsilon_f + \epsilon_f' = \epsilon_f - \frac{\epsilon_f f_f}{f_f - \epsilon_f} = \epsilon_f \left(1 - \frac{\frac{f_f}{c}}{\frac{f_f}{c} - \frac{\epsilon_f}{c}} \right) \tag{26}$$

In figure 9, note that ϵ_f' is an image distance on the object side of the lens and is inherently negative.

In order for the effect on the final image to be negligible, the image must remain within the camera depth of field, thus yielding the requirement that

$$\Delta \leq \frac{\Delta l_c}{2} \tag{27a}$$

By substituting equations (26) and (3) into (27a), and by solving for ϵ_f/c, the limiting value for ϵ_f/c becomes

$$\frac{\epsilon_f}{c} \leq \frac{\left(\frac{\beta c}{D_c}\right)\left(\frac{l_f'}{c}\right)^2 + \sqrt{\left[\left(\frac{\beta c}{D_c}\right)\left(\frac{l_f'}{c}\right)^2\right]^2 - 4\left(\frac{\beta c}{D_c}\right)\left(\frac{l_f'}{c}\right)^2 \frac{f_f}{c}}}{2}$$

However, holding c constant implies that f_f is a function of l_f'/c as discussed previously in the section entitled "Transverse magnification"; so ϵ_f/c is better expressed as

$$\frac{\epsilon_f}{c} \leq \frac{\left(\frac{\beta c}{D_c}\right)\left(\frac{l_f'}{c}\right)^2 + \sqrt{\left(\frac{\beta c}{D_c}\right)\left(\frac{l_f'}{c}\right)^2 - 4\left(\frac{\beta c}{D_c}\right)\left(\frac{l_f'}{c}\right)^2\left(\frac{l_f'}{c}\right)\left(1 - \frac{l_f'}{c}\right)}}{2} \tag{27b}$$

The equality in equation (27b) is plotted in figure 9(b). Shown is the variation of the normalized misplacement error ϵ_f/c plotted against the normalized field-lens position

l'_f/c for various values of f_f/c and a typical value of $\beta c/D_c$. Errors below these curves are acceptable, but errors above these curves would lead to significant blurring.

Auxiliary lens.- Small displacements of the auxiliary lens from its intended position have the effect of misplacing the intermediate image away from the field lens. The effect of the field lens on a slightly misplaced image is small as long as the misplacement is small; the final image will be blurred only if the misplaced intermediate image does not lie within the depth of field of the camera.

The intermediate image may be moved by one-half of the camera depth of field to remain in acceptable focus; that is,

$$\Delta'_f < \frac{\Delta l_c}{2}$$

where Δ'_f is the misplacement of the image formed by the field lens of the misplaced intermediate image and where Δl_c is given by equation (3). For small errors in placement, the field lens has little effect; if Δ'_a represents the conjugate distance to Δ'_f (that is, the distance to the field-lens image of the auxiliary-lens image), then

$$\Delta'_a = \frac{\Delta'_f f_f}{\Delta'_f - f_f} \approx \Delta'_f$$

A misplacement ϵ_a in the auxiliary-lens position (shown in fig. 10) changes the object conjugate l_a to

$$\tilde{l}_a = l_a - \epsilon_a$$

The image conjugate becomes

$$\tilde{l}'_a = \frac{\tilde{l}_a f_a}{l_a - f_a}$$

and Δ'_a is given by

$$\Delta'_a = \tilde{l}'_a - \epsilon_a - l'_a$$

Thus, since $l'_a = l_f = c - l'_f$ and $l_a = \frac{\tilde{l}'_a f_a}{l'_a - f_a}$, then

$$\Delta_f' \approx \Delta_a'$$

$$= \frac{(l_a - \epsilon_a) f_a}{l_a - \epsilon_a - f_a} - \epsilon_a - l_a'$$

$$= \frac{\left\{\left[\tilde{l}_a' f_a / (l_a' - f_a)\right] - \epsilon_a\right\} f_a}{\left[\tilde{l}_a' f_a / (l_a' - f_a)\right] - \epsilon_a - f_a} - \epsilon_a - \frac{\tilde{l}_a' f_a}{l_a' - f_a}$$

$$= \frac{\left\{\left[\left(1 - \frac{l_f'}{c}\right)\frac{f_a}{c} \Big/ \left(1 - \frac{l_f'}{c} - \frac{f_a}{c}\right)\right] - \frac{\epsilon_a}{c}\right\}\frac{f_a}{c}}{\left[\left(1 - \frac{l_f'}{c}\right)\frac{f_a}{c} \Big/ \left(1 - \frac{l_f'}{c} - \frac{f_a}{c}\right)\right] - \frac{\epsilon_a}{c} - \frac{f_a}{c}} - \frac{\epsilon_a}{c} - \frac{\left(1 - \frac{l_f'}{c}\right)\frac{f_a}{c}}{1 - \frac{l_f'}{c} - \frac{f_a}{c}}$$

This expression is not soluble for ϵ_a/c in terms of l_f'/c, but the numerical solution is shown in figure 10(b) for typical values of f_a/c and $\beta c/D_c = 0.07$.

EVALUATION OF PERFORMANCE, CONSTRAINTS, AND REQUIREMENTS FOR THE VIKING LANDER CAMERA

The foregoing analysis has revealed a variety of constraints imposed on the compound quasi-microscope performance by the facsimile-camera line-scan mirror, by requirements imposed on the facsimile-camera design, and by strict tolerances imposed on the auxiliary- and field-lens locations. To render the trade-off between performance, constraints, and requirements more tractable, it is necessary to make some concrete assumptions about camera parameters. The Viking lander camera and auxiliary-lens parameters considered here as a specific example are listed in table I.

It may be noted that a 3-cm focal-length auxiliary lens was found in reference 9 to provide the highest realizable resolution (20 μm) for the Viking lander camera in the simple quasi-microscope mode, but it has an almost unacceptable small number of unvignetted pixels in the central line scan.

Based on these assumptions, figure 11 presents the constraints, performance, and requirements of figures 4, 6, 7(c), 8, 9(b), and 10(b). Figure 11(a) has the vignetting constraints imposed by design 1, and figure 11(b) has those imposed by design 2. In

each figure, the first graph shows the relationship between field-lens size (vertical axis) and position (horizontal axis) and the number of unvignetted pixels available to the camera.

In figure 11(a), points lying under the vignetting-limit curves have coordinates satisfying the design 1 vignetting condition. Since these points also lie to the right of the curved-field limit, the curved-field constraint is not an important consideration for the given assumptions. In figure 11(b), only those points lying to the right of the vignetting-limit curves which correspond to the chosen auxiliary-lens diameter represent designs which satisfy the design 2 vignetting constraint. Again, those designs not permitted because of the curved-field limit also violate the vignetting condition.

Other than the vignetting limits, figures 11(a) and 11(b) are identical. In each, the second graph shows the position of the photosensor inside the camera in multiples of the camera focal length. (In the normal facsimile camera the normal imaging detector would be located near the lens focal point.) Below this graph are curves for pixel diameter (resolution) and depth of field, taken from figure 4. Finally, the axial tolerances for both auxiliary and field lenses are shown in the fifth and sixth graphs, respectively.

It is now possible to evaluate the trade-off between design configurations 1 and 2. It has already been noted that design 1 offers higher resolution at the expense of lower sensitivity. From figure 11(a) it can be seen that, in addition, the number of picture elements available to the camera is smaller for design 1. The physical reason is that the mirror must rotate through an appreciable angle in order to scan the entire field lens when the field lens is close by, and, therefore, the auxiliary-lens image reaching the edge of the camera limits the unvignetted field. Since the number of pixels covered is directly proportional to the angle through which the mirror moves, the number of pixels is limited. In the Viking example of figure 11(a), the maximum number of pixels per central line scan available for design 1 and for a 2.0-cm auxiliary lens is about 175. With this number of pixels, the camera's noise-equivalent radiance would be increased by the ratio $(D_i/D_c)^2$, or in this case about 70 percent. However, the pixel diameter, about 2 μm, is far smaller than that which could be obtained with design 2. By contrast, design 2 offers up to 275 pixels in the center line scan, thus yielding a total of 2×10^4 pixels in the whole field; unfortunately, such a large field would require an 8.0-cm field lens and give a pixel diameter of only 12 μm.

This example clearly illustrates that the trade-off between resolution and field has not been completely avoided in the compound quasi-microscope design, though it has been relaxed considerably from the simple design.

For design 1, there is an absolute limitation on field for a given auxiliary-lens diameter. On the other hand, for design 2 there is no absolute limit, since the field lens can be moved as far from the camera as necessary; however, the gain in the number of unvignetted pixels must be paid for by loss of magnification.

It should be noted that the foregoing study is based on a first-order analysis with thin, perfect lenses considered. In a real system, consideration must be given to more practical problems. Among these are questions of image curvature introduced by the field lens and the desirability of deliberately displacing the field lens from the image plane to avoid imaging the dust collected on its surfaces. Designs based on figure 11 must be chosen with such effects in mind.

CONCLUDING REMARKS

In order to overcome the limitations on resolution and object field of a recently proposed quasi-microscope concept, which consists of a facsimile camera and an auxiliary lens as a magnifier, a compound quasi-microscope was analyzed which includes a field lens between camera and auxiliary lens. This analysis revealed that pixel diameters of about 2 μm or fields up to 2×10^4 pixels per image might be obtained with the compound design, as compared with pixel diameters of 20 μm and fields of 10^3 pixels per image for the previous design.

Other than the accompanying decrease in depth of field, the primary expenses for these improvements were the additional complexity of a field lens, the considerably increased required focus range for the facsimile camera, and a tighter tolerance on the placement of the auxiliary lens with respect to the camera. Curves have been presented which permit trade-offs to be made between the performances achievable with this design and the resultant requirements.

Langley Research Center,
National Aeronautics and Space Administration,
Hampton, Va., December 10, 1973.

APPENDIX

EVALUATION OF THE DISTANCE ξ

In evaluating the distance ξ, consider figure 7(b), which reproduces part of figure 7(a) on a larger scale. The distance ξ in design 1 is that distance measured on the camera-lens aperture between the ray leaving the top rim of the field lens and passing through the lower edge of the auxiliary-lens image and a perpendicular to that image at its lower edge. Alternately, in design 2, ξ is the distance on the camera-lens aperture between the ray leaving the lower rim of the field lens and passing through the upper edge of the auxiliary-lens image and a perpendicular to that image at its upper edge.

In figure 7(b), note that ξ is one side of a triangle which is determined by the angles ϕ and $\frac{\pi}{2} + \theta$ and the side between these angles $\frac{D_i}{2} \tan \theta$. Then, from the law of sines on this triangle,

$$\xi = \left(\frac{D_i}{2} \tan \theta\right) \frac{\sin \phi}{\sin \chi}$$

where

$$\chi = \pi - \phi - \left(\frac{\pi}{2} + \theta\right) = \frac{\pi}{2} - \phi - \theta$$

Then,

$$\xi = \frac{D_i}{2} \frac{\tan \theta \sin \phi}{\cos(\phi + \theta)}$$

where θ is the half field angle and ϕ is the half angular extent of the camera lens from the extreme field point. (See fig. 7.) Since ϕ will be only a few degrees for any reasonable design, it can be assumed that $\sin \phi = \phi$ and $\cos(\theta + \phi) = 1$. Further, the product $\phi \tan \theta$ is much less than $\tan \theta$; therefore,

$$\xi \approx \frac{D_i}{2} \phi \tan \theta \ll K' \tan \theta$$

REFERENCES

1. Selivanov, A. S.; Govorov, V. N.; Titov, A. S.; and Chemodanov, V. P.: Lunar Station Television Camera. Contract NAS 7-100, Reilly Translations, 1968. (Available as NASA CR-97884.)

2. Cherkasov, I. I.; Kemurdzhian, A. L.; et al.: First Panoramas of "LUNA-13" – Determination of Density and Mechanical Strength of Lunar Surface Layer at the Landing Site of the Automatic Station "LUNA-13." NASA CR-88874, 1967.

3. Brereton, R. G.; Burke, J. D.; Coryell, R. B.; and Jaffe, L. D.: Lunar Traverse Missions. JPL Quart. Tech. Rev., vol. 1, no. 1, Apr. 1971, pp. 125-137.

4. Surveyor Project Staff: Surveyor Project Final Report. Pt. I. Project Description and Performance – Volume I. Tech. Rep. 32-1265, Jet Propulsion Lab., California Inst. Technol., July 1, 1969. (Available as NASA CR-105302.)

5. Mutch, T. A.; Binder, A. B.; Huck, F. O.; Levinthal, E. C.; Morris, E. C.; Sagan, Carl; and Young, A. T.: Imaging Experiment: The Viking Lander. Icarus, vol. 16, no. 1, Feb. 1972, pp. 92-110.

6. Greene, V. W.; Landgren, D. A.; Mullin, D. D.; and Peterson, R. E.: Microscopic System for Mars Study Program. Rep. No. 2326 (Contract JPL 950123), General Mills Electronics Div., Aug. 14, 1962. (Available as NASA CR-51538.)

7. Loomis, Alden A.: A Lunar and Planetary Petrography Experiment. Tech. Rep. No. 32-785, Jet Propulsion Lab., California Inst. Technol., Sept. 1, 1965.

8. Soffen, Gerald A.: Extraterrestrial Optical Microscopy. Appl. Opt., vol. 8, no. 7, July 1969, pp. 1341-1348.

9. Huck, Friedrich O.; Sinclair, Archibald R.; and Burcher, Ernest E.: First-Order Optical Analysis of a Quasi-Microscope for Planetary Landers. NASA TN D-7129, 1973.

10. Huck, Friedrich O.; and Lambiotte, Jules J., Jr.: A Performance Analysis of the Optical-Mechanical Scanner as an Imaging System for Planetary Landers. NASA TN D-5552, 1969.

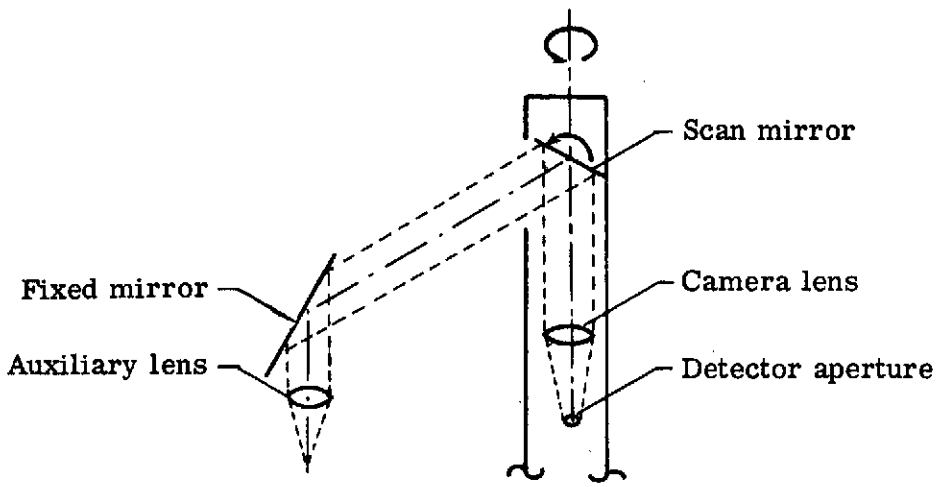

(a) Basic configuration.

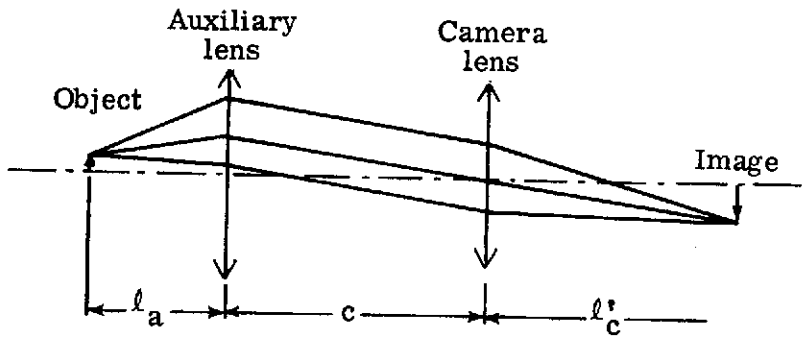

(b) Optical geometry.

Figure 1.- Simple quasi-microscope.

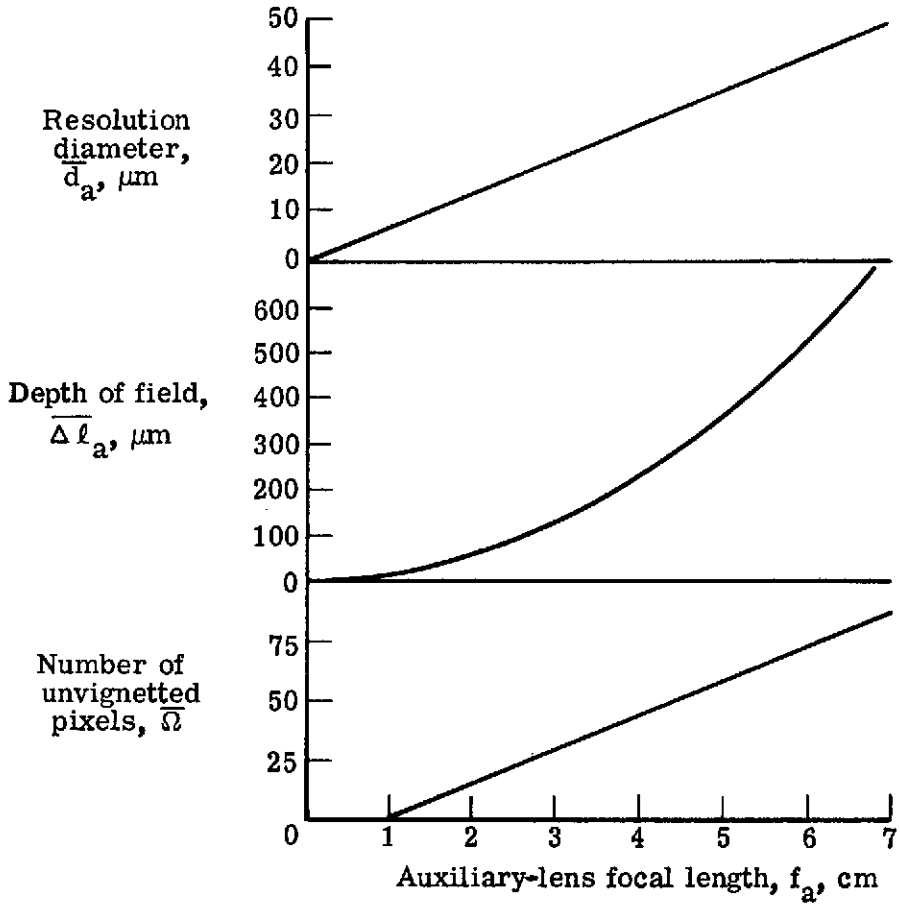

Figure 2.- Simple quasi-microscope performance for Viking lander camera parameters (adapted from ref. 9).

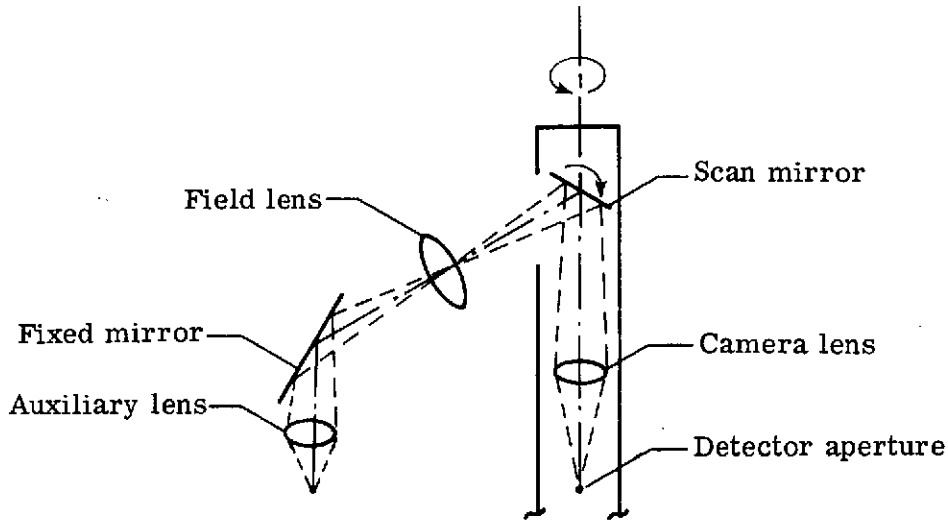

(a) Basic configuration.

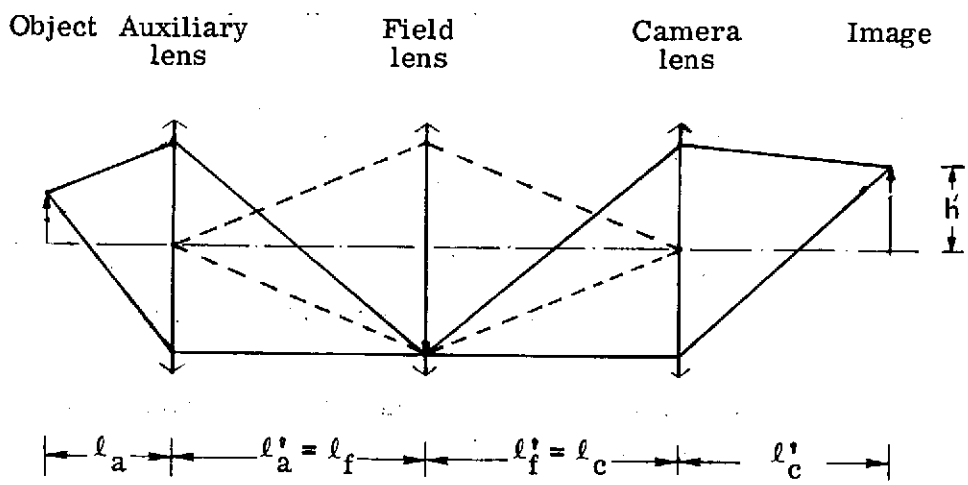

(b) Optical geometry.

Figure 3.- Compound quasi-microscope.

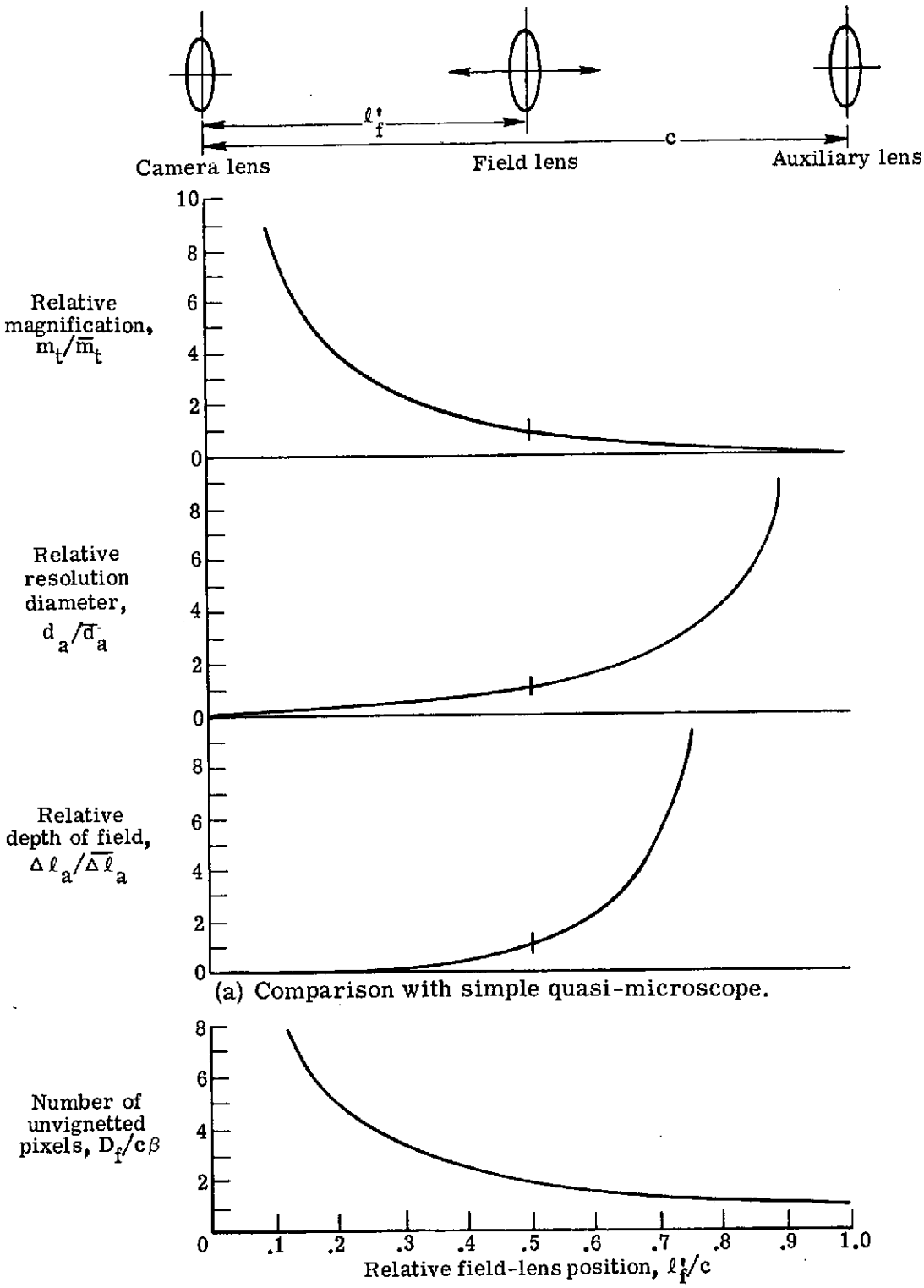

(a) Comparison with simple quasi-microscope.

(b) Number of unvignetted pixels.

Figure 4.- Compound quasi-microscope performance.

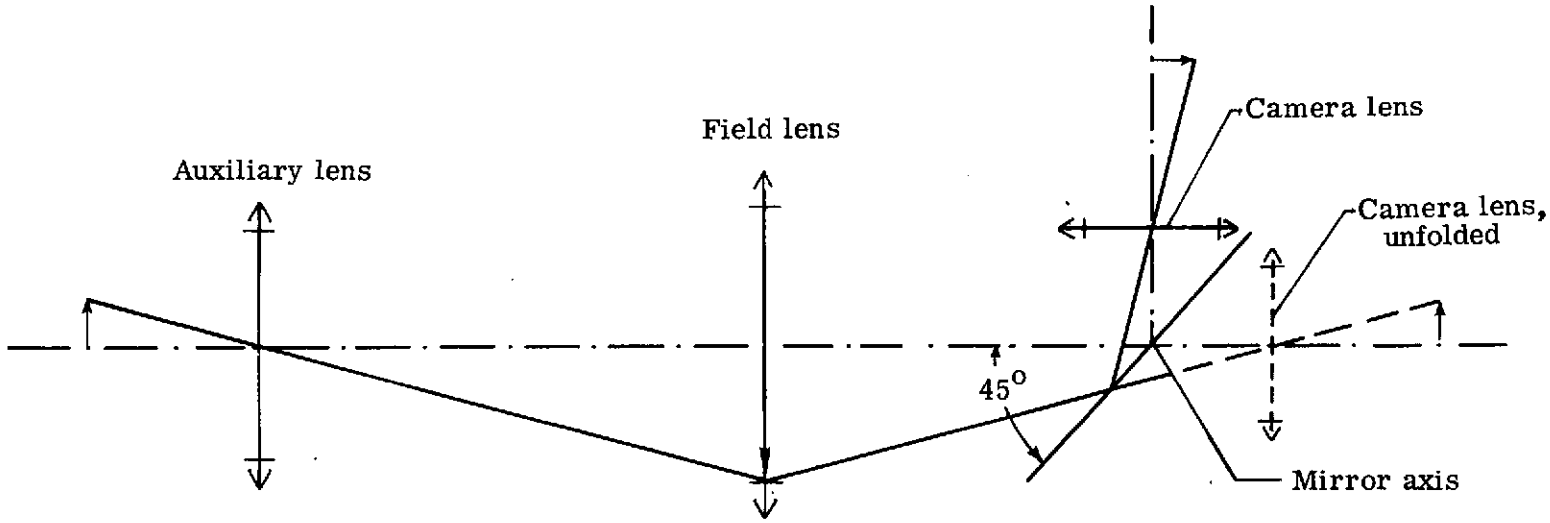

(a) Simplified model used for performance analysis.

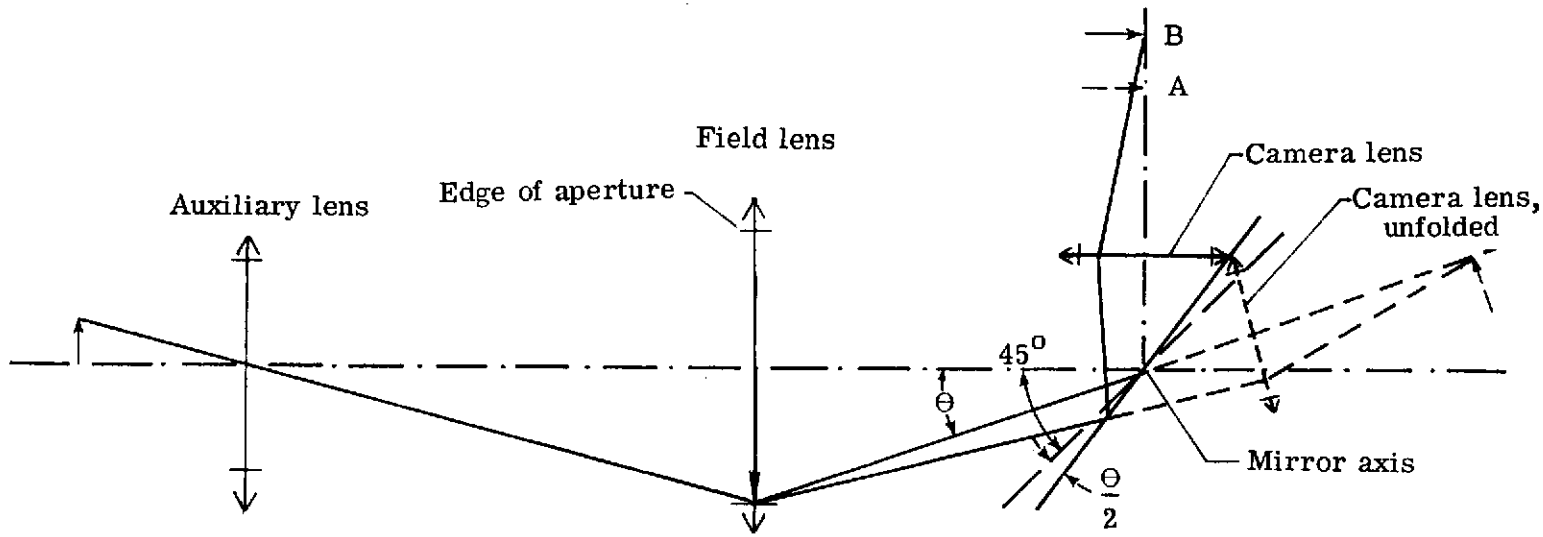

(b) Corrected model used in constraint analysis.

Figure 5.- Unfolding the optical system.

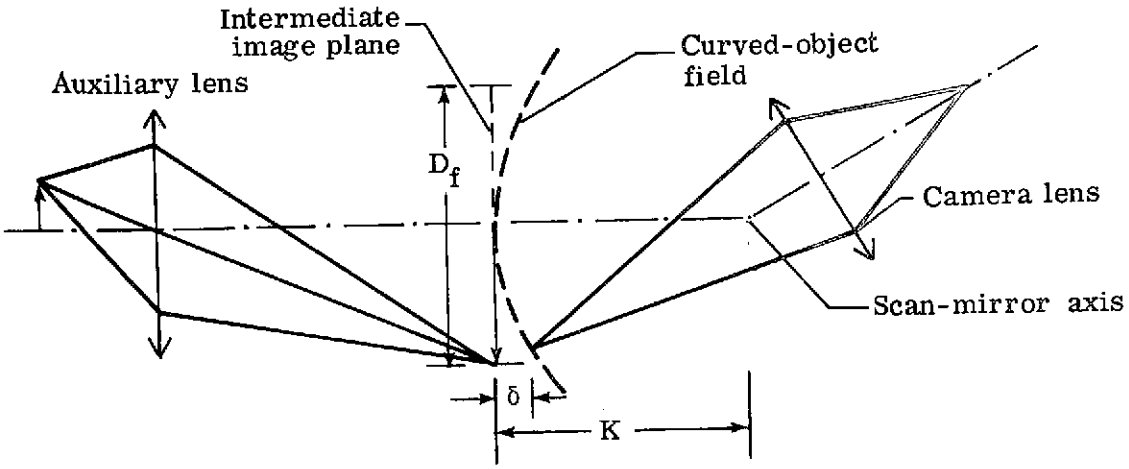

(a) Optical geometry. Field lens was omitted from drawing.

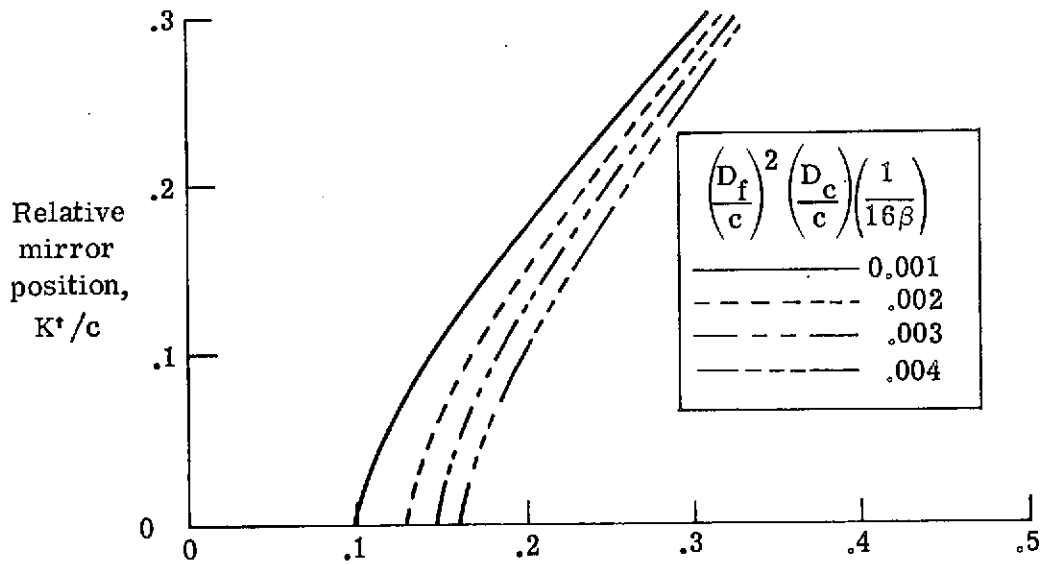

(b) Limits imposed on field-lens position.

Figure 6.- Constraint imposed by curved-object field.

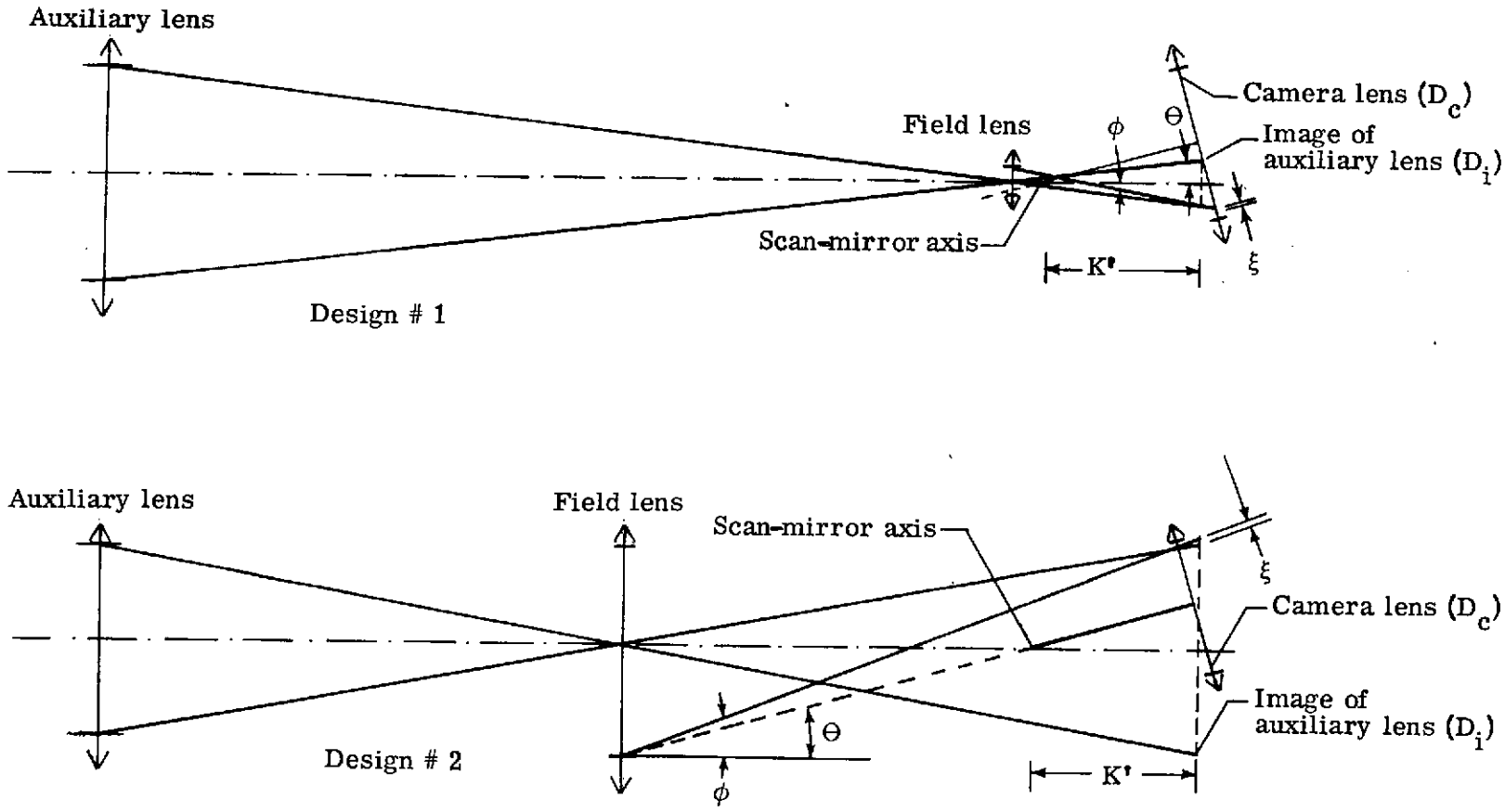

(a) Optical geometry.

Figure 7.- Constraint imposed by field vignetting.

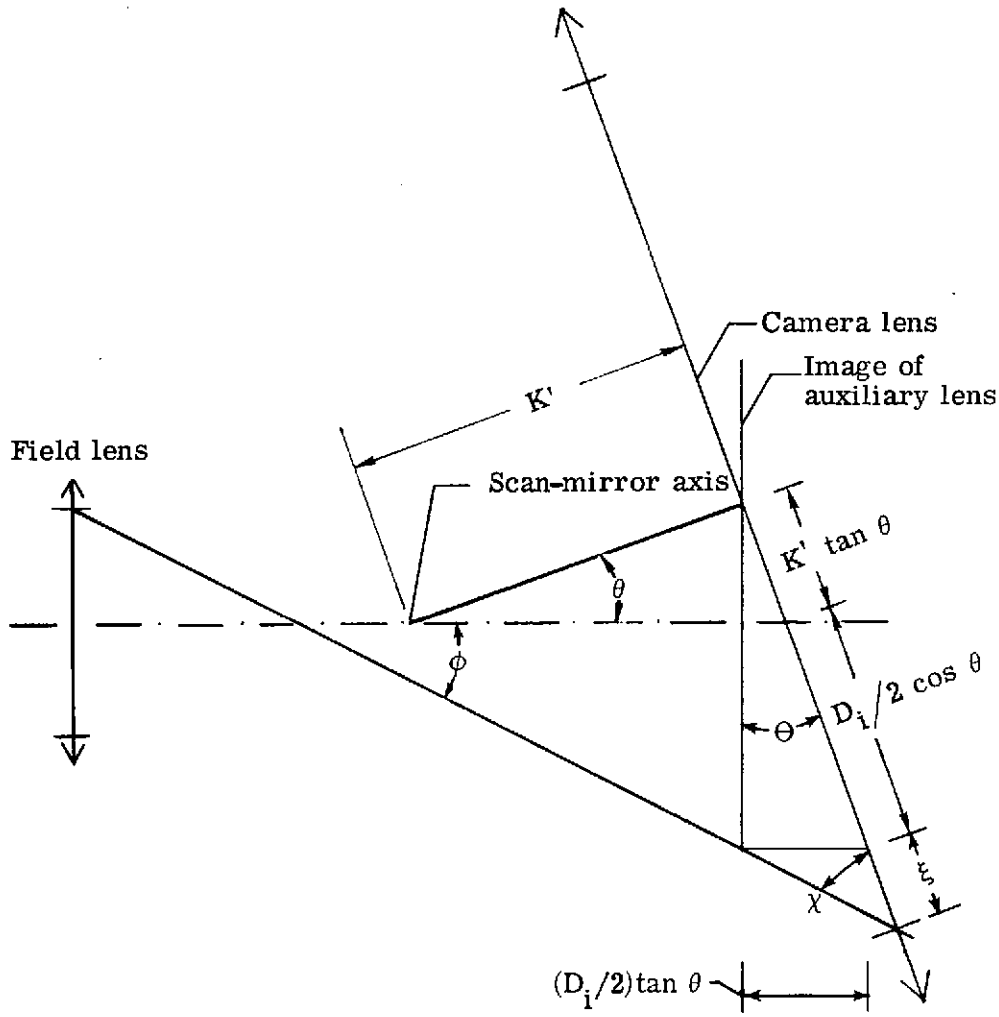

(b) Detail showing design 1 vignetting.

Figure 7.- Continued.

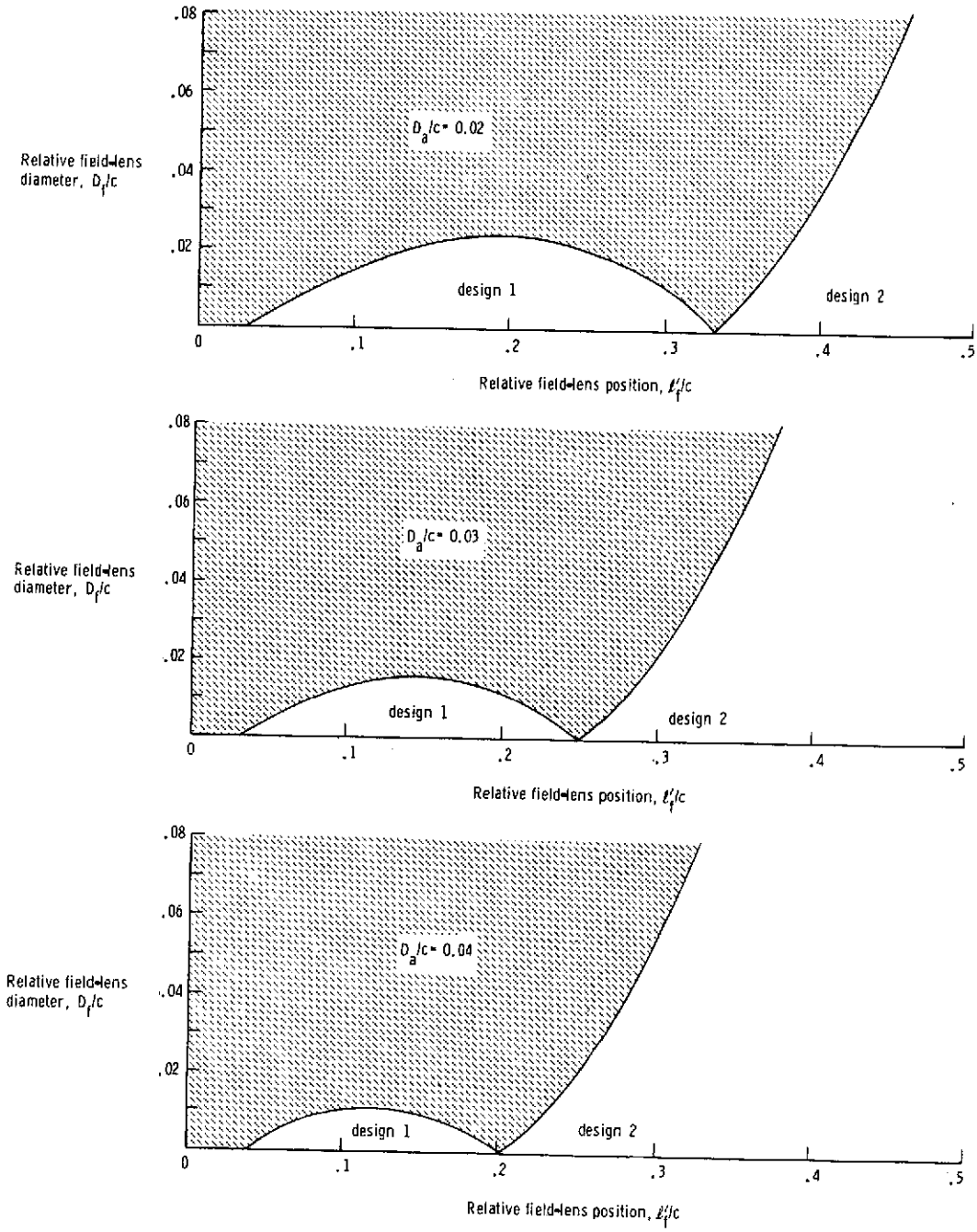

(c) Limits imposed on relative field-lens position. Shaded areas indicate forbidden combinations of field-lens diameter and position.

Figure 7.- Concluded.

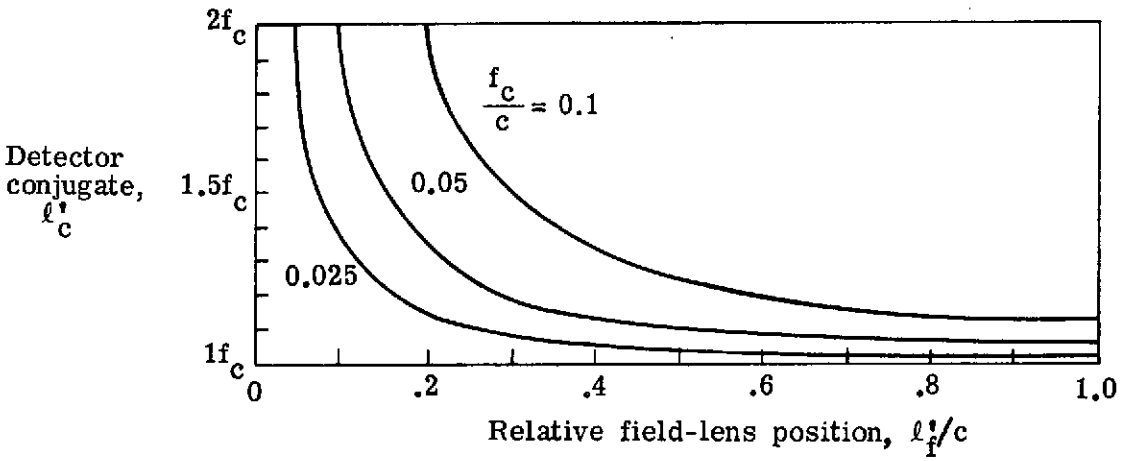

Figure 8.- Camera photodetector conjugate plotted against field-lens position.

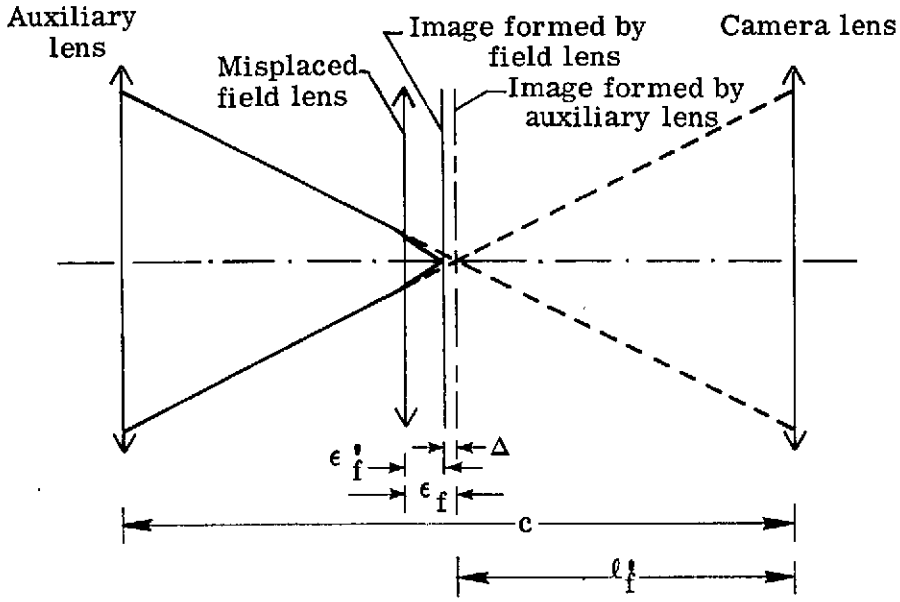

(a) Optical geometry.

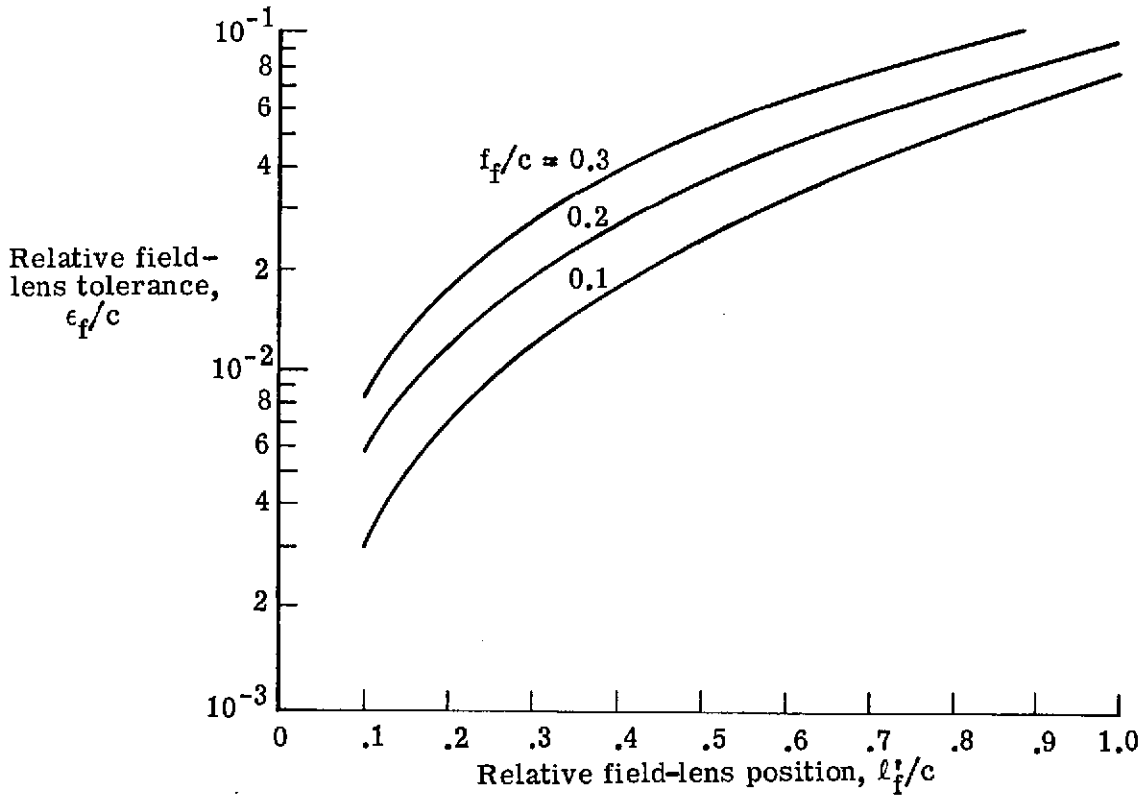

(b) Field-lens misplacement tolerance. $\beta c/D_c = 0.07$.

Figure 9.- Misplacement of field lens.

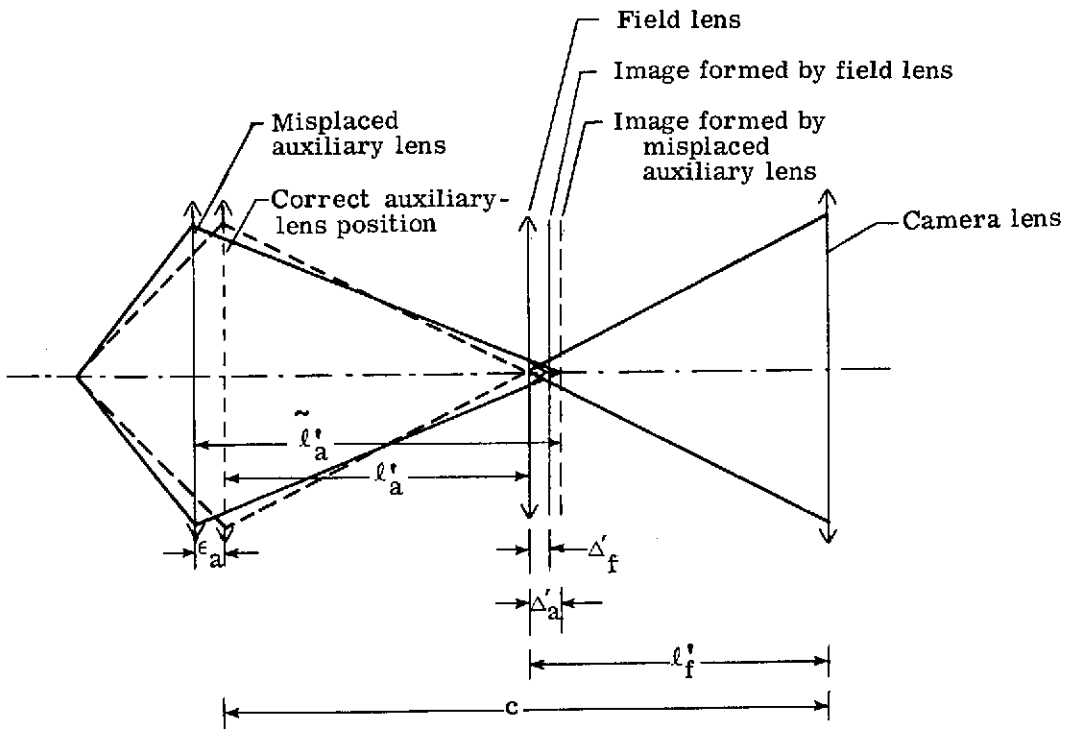

(a) Optical geometry.

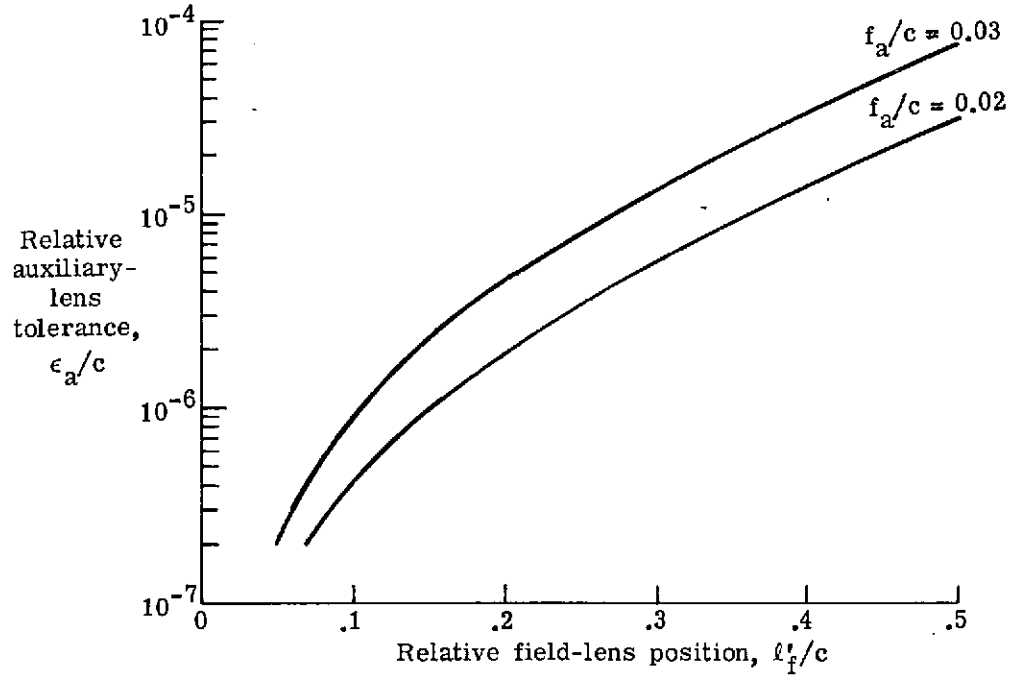

(b) Auxiliary-lens misplacement tolerance. $\beta c/D_c = 0.07$.

Figure 10.- Misplacement of auxiliary lens.

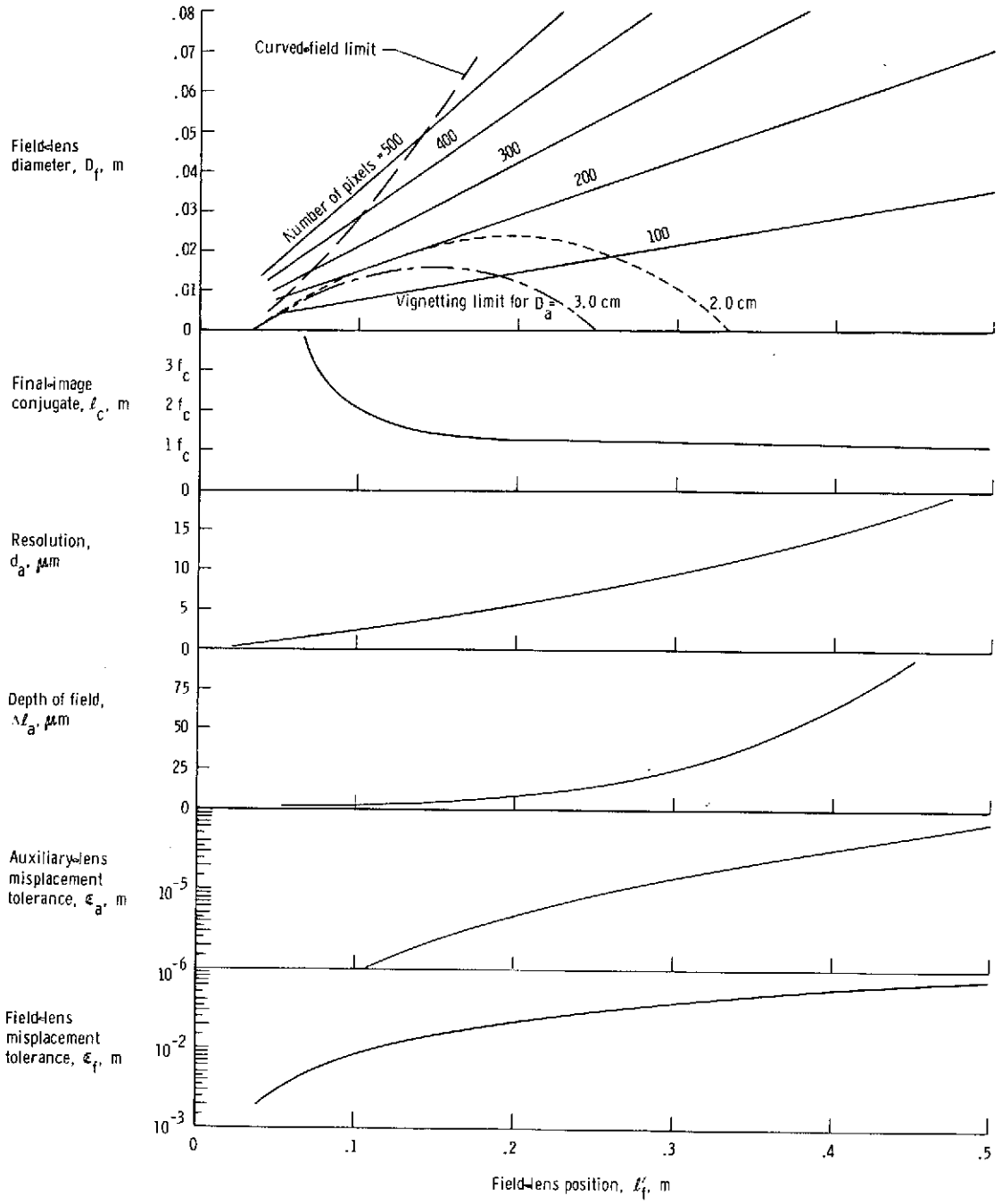

(a) Design 1.

Figure 11.- Nomograph of compound quasi-microscope performance and constraints for Viking lander camera parameters. f_a = 3.0 cm.

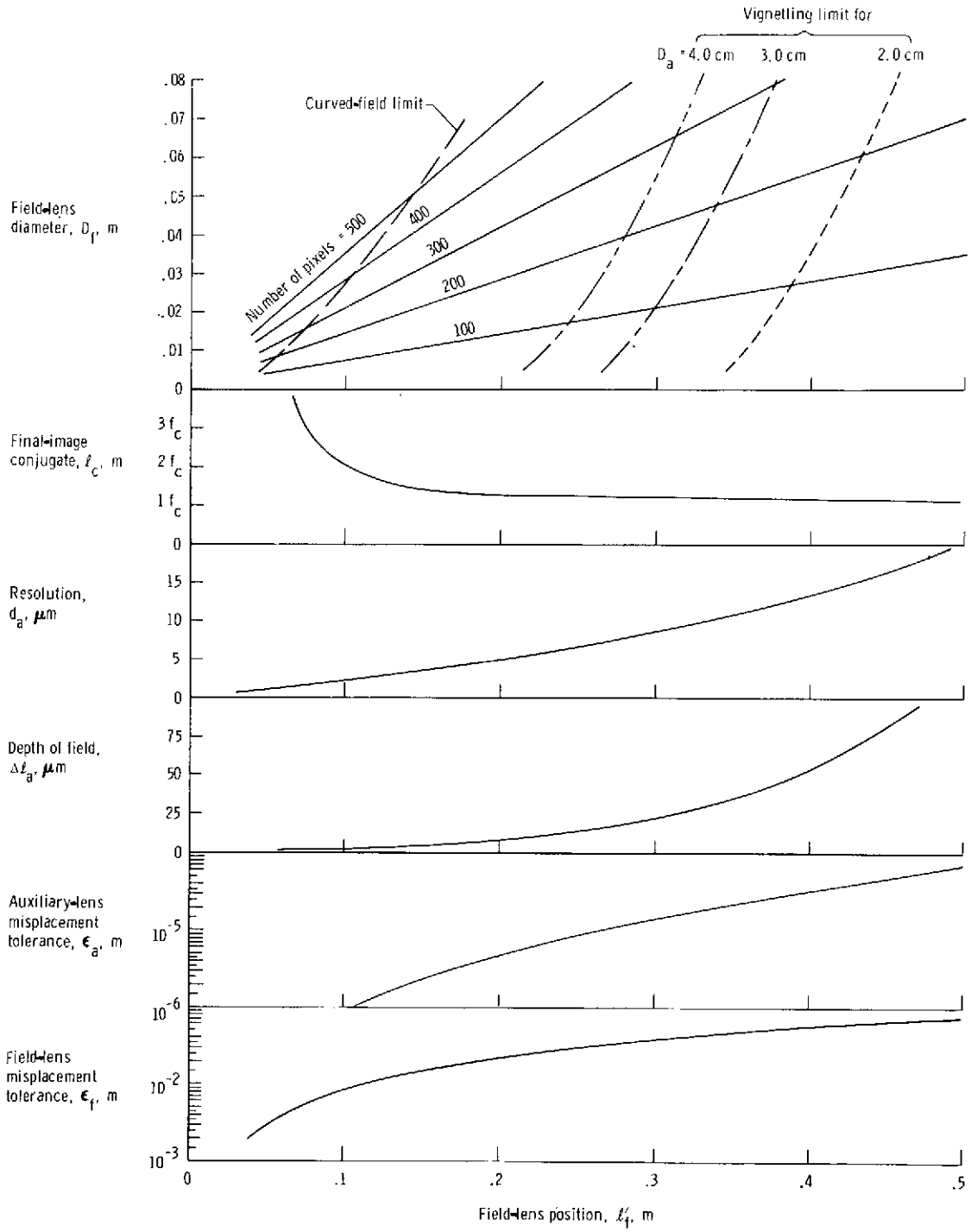

(b) Design 2.

Figure 11.- Concluded.